Electron capture, electron loss, and deexcitation of fast $H(2^2S)$ and $H(1^2S)$ atoms in collisions with molecular hydrogen and inert gases

F. Roussel, P. Pradel, and G. Spiess
Service de Physique Atomique, Centre d'Etudes Nucléaires de Saclay, Boite Postale No. 2, 91190 Gif-sur-Yvette, France
(Received 31 May 1977)

Collisions of ground-state (1^2S) and metastable (2^2S) hydrogen atoms with rare gases and molecular hydrogen have been studied in the energy range 0.5–3.0 keV. For an acceptance angle of 55 mrad, the electron loss and the electron-capture cross sections of both $H(1^2S)$ and $H(2^2S)$ have been measured and compared with previous experimental values. The deexcitation cross section for $H(2^2S)$ has been deduced with the help of previously measured total-quenching cross sections for $H(2^2S)$. The ratio of the electron-capture cross sections for $H(2^2S)$ relative to $H(1^2S)$ is found to be very large for argon at low energies. The effects of large-angle scattering and of highly excited states of H are discussed.

I. INTRODUCTION

Collision processes occurring during the passage of a fast metastable or ground-state H atom beam through gas targets are of both fundamental interest and practical use. For example, electron-loss processes of fast hydrogen atoms are of fundamental importance in proton auroras, whereas knowledge of electron-capture processes by metastable hydrogen is necessary when considering possible sources for polarized negative hydrogen ions, such as was discussed in the proposal of Donnally and Sawyer.[1]

Until now very few absolute measurements have been reported for energies below 2 keV, especially for collisions involving $H(2^2S)$ atoms. Stier and Barnett[2] determined charge-exchange cross sections for hydrogen atoms and ions in various gases in the energy range 3–200 keV. In 1960, Curran and Donahue[3] measured electron-capture and -loss cross sections for ground-state hydrogen atoms in molecular hydrogen. McClure[4] presented in 1964 measurements of electron loss and capture from ground-state H atoms in molecular hydrogen in the energy range 2–120 keV. Williams[5] measured in 1967 electron-capture and -loss cross sections for 2–50 keV hydrogen atoms incident upon hydrogen and the inert gases. In 1972, Dose and Gunz[6,7] published measurements of electron-loss cross sections for metastable hydrogen atoms in collisions with Ar, H_2, N_2, and O_2 in the energy range 2–60 keV, and of electron-capture cross sections for metastable H atoms in Ar, N_2, and O_2 in the energy range 1.4–8 keV. Spiess, Valance, and Pradel[8] gave values of electron-loss cross sections for $H(2^2S)$ in collisions with the rare gases, molecular hydrogen, and nitrogen at 2.5 keV. These are the only previous determinations of electron capture and loss by metastable hydrogen atoms in our energy range. More recently, Smith *et al.*[9] measured electron-loss cross sections for ground-state hydrogen atoms in collisions with atmospheric gases in the energy range 0.25–5 keV. Noda[10] found electron-loss cross sections for ground-state hydrogen molecules in the energy range 0.2–5 keV, while Morgan *et al.*[11] measured electron-loss and -capture cross sections for $H(2^2S)$ in xenon for the energy range 2–25 keV.

Theoretical calculations have been carried out in the 0.5–3.0 keV energy range by Levy[12,13] for electron-loss processes from ground-state and metastable H atoms in collisions with rare gases. Recently, Olson[14] calculated electron-capture cross sections for metastable hydrogen atoms in collisions with argon, krypton, and xenon.

In listing the reactions involving the metastable and ground-state H atom, we will use the following notation: the subscript g refers to $H(1^2S)$, m to $H(2^2S)$, + to H^+, and − to H^-. For a ground-state H atom beam incident on a target gas X, in our energy range, the following reactions (with cross sections σ) may occur:

$$H(1^2S)+X \rightarrow H^+ + X + e^- , \quad \sigma_{g+} ; \tag{1}$$

$$H(1^2S)+X \rightarrow H^- + X^+ , \quad \sigma_{g-} ; \tag{2}$$

$$H(1^2S)+X \rightarrow H(2^2S)+X , \quad \sigma_{gm} . \tag{3}$$

A metastable $H(2^2S)$ beam may be destroyed by the following reactions:

$$H(2^2S)+X \rightarrow H^+ + X + e^- , \quad \sigma_{m+} ; \tag{4}$$

$$H(2^2S)+X \rightarrow H^- + X^+ , \quad \sigma_{m-} ; \tag{5}$$

$$H(2^2S)+X \rightarrow H(1^2S)+X , \quad \sigma_{mg} ; \tag{6}$$

where deexcitation to the ground state may occur either directly or via an adjacent excited state.

We report here measurements of the charge-exchange cross sections σ_{g+}, σ_{g-}, σ_{m+}, σ_{m-}, and deexcitation cross sections σ_{mg} for hydrogen mole-

cules and the inert gases for H energies in the range 0.5–3.0 keV.

II. EXPERIMENTAL APPROACH

A. Apparatus

The apparatus previously described in detail[15,16] has been modified in order to increase the acceptance angles of the detectors. A schematic diagram is shown in Fig. 1. It consists basically of a beam of fast H atoms in the ground state with a large admixture in the metastable $2\,^2S$ state. The beam passes through a gas target, after which the charged components created are separated from the neutral beam and detected. The electron-loss and electron-capture cross sections at a given energy are derived from the yield of H^+ and H^- for a given target gas pressure.

A hydrogen-ion beam is extracted from a duoplasmatron source and is focused by an Einzel lens. It is magnetically mass analyzed and suitably collimated. The proton beam so created enters a cell containing cesium vapor. The H^+ beam is partially neutralized in the thin Cs target where quasiresonant charge-exchange processes occur. The beam emerging from the Cs target contains H^+ and H^- ions, and H atoms in the $1\,^2S$ and $2\,^2S$ states. H atoms formed in the radiative $2\,^2P$ state essentially decay immediately to the $1\,^2S$ state, while those formed in the $2\,^2S$ state remain in this state, as the field free lifetime is very long (0.14 sec). After traversing the cell, the entire beam passes between two electrostatic deflection plates which remove the ions with a weak transverse electric field of 1.5–4.5 V/cm (depending on the beam energy), sufficient for removing all the ions, while producing minimal quenching (<2%) of the metastable H atoms. If desired the deflection plates can also be used to quench the metastable atoms in the $2\,^2S$ state before they enter the target cell by applying a field of 150 V/cm which is sufficient to quench essentially all the metastable atoms by Stark effect.

Thus, after passage through this region, the neutral beam consists of H atoms in the $1\,^2S$ state with a large admixture in the metastable $2\,^2S$ state (between 25% and 50%[15,17]) and a small fraction in higher excited states. In order to test the effect of these long-lived excited atoms upon our cross-section measurements, two grids, 1 mm apart, have been placed perpendicular to the beam axis, just in front of the ion sweeping plates. A strong electric field (15 kV/cm) applied between these two grids will almost entirely ionize atoms in states with $n \geq 15$ (see discussion in Sec. III E). About 1 m downstream from the Cs target is the gas target cell where electron-loss and electron-capture collisions are studied. This distance is long enough so that, even at 3 keV where the travel time for the atoms is about 1.3 μsec, any H atoms with $3 \leq n \leq 6$, formed in the Cs target, would have time to decay to the $1\,^2S$ state.

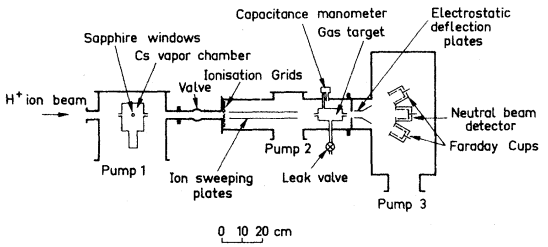

FIG. 1. Schematic diagram of the apparatus.

The H^+ and H^- ions created in the gas cell can be separated by electrostatic deflection and measured with suppressed Faraday cups, symmetrically located about the beam axis. The neutral beam intensity is measured with a detector that utilizes secondary-electron emission. The target gas cell has a 15-cm effective length (length of central part plus one end tube), an entrance aperture 5 mm in diameter, and an exit aperture 9 mm in diameter. This defines an acceptance angle (half angle) for the detection of H^+, H^-, and neutral H atoms of 50 mrad. If, however, the end tubes are reversed, so that they are inside the gas cell, the effective length of the cell is shortened to 10.4 cm, and the acceptance angle then becomes 55 mrad. As the scattering is important, even for angles greater than 50 mrad, this second possibility was always used. The pressure of the target gas in the cell is measured by a capacitance manometer (MKS Baratron type 170 M-7) with a heated head having a full scale range of 1 Torr, calibrated by the manufacturer. The error in the absolute pressure calibration is about 3%, with a typical target gas pressure being 2×10^{-4} Torr. The background pressure in the vacuum system is 2×10^{-7} Torr.

B. Experimental method

1. Electron-loss and electron-capture cross sections for H($1\,^2S$) atoms

When the target-gas density is sufficiently low to ensure that only single collisions occur, and the metastable atoms are quenched before reaching the gas cell, the resulting H^+ and H^- intensities measured after passing through the target are

$$I^+(\pi) = (I_g^0 + I_m^0)(1 - e^{-\sigma_{g+}\pi}) = I^0(1 - e^{-\sigma_{g+}\pi}) , \tag{7}$$

$$I^-(\pi) = (I_g^0 + I_m^0)(1 - e^{-\sigma_{g-}\pi}) = I^0(1 - e^{-\sigma_{g-}\pi}) , \tag{8}$$

where I_g^0 and I_m^0 are the intensities of beam atoms in the $1\,^2S$ state and $2\,^2S$ state, respectively, in the

beam before the quenching region. I^0 is the total neutral intensity entering the gas cell in the $1\,^2S$ state and π is the effective target thickness: $\pi = n \times L$, where n is the density of the target and L the effective target length. The quantities σ_{g^+} and σ_{g^-} can be derived from Eqs. (7) and (8):

$$\sigma_{g^+} = -\frac{1}{\pi}\ln\left(1 - \frac{I^+(\pi)}{I^0}\right), \tag{9}$$

$$\sigma_{g^-} = -\frac{1}{\pi}\ln\left(1 - \frac{I^-(\pi)}{I^0}\right). \tag{10}$$

The neutral current I^0 incident on the gas cell cannot be measured when gas is in the cell and has to be estimated by a calculated value $I^0_{\rm calc}$. In order to calculate $I^0_{\rm calc}$, we alternately measured $I^0(0)$, the neutral beam intensity without gas in the cell, and $I^0(\pi)$, the neutral beam intensity with gas in the cell when atoms in the $2\,^2S$ state are quenched. By doing this 15 times, we can then define an average neutral correction factor:

$$\langle C\rangle = \langle I^0(\pi)\rangle / \langle I^0(0)\rangle . \tag{11}$$

This factor $\langle C\rangle$ is simply the sum of those elastic and inelastic scattering processes which reduce the transmitted neutral current when gas is in the cell. $\langle C\rangle$ varies from 0.96 to 0.99. We then calculate $I^0_{\rm calc}$ by

$$I^0_{\rm calc} = I^0(\pi)/\langle C\rangle . \tag{12}$$

Because a secondary electron current is measured, it is necessary to calibrate the neutral particle detector in order to obtain $I^0(\pi)$. The new neutral detector has been calibrated in the same manner as previously described.[15,16] Although this new detector was made from the same material ("dirty" stainless steel) as the previous one, the values for γ_g are 20% lower than the values reported elsewhere.[15] This is probably due to pollution of the old detector by cesium. The measured value $I^0(\pi)_{\rm mes}$ of $I^0(\pi)$ is

$$I^0(\pi)_{\rm mes} = \gamma_g I^0(\pi) . \tag{13}$$

For a given target thickness π, we measured simultaneously $I^0(\pi)_{\rm mes}$, $I^+(\pi)$, and $I^-(\pi)$ 10 times each. Averaging Eqs. (9) and (10) over the set of data and using Eqs. (12) and (13) to estimate I^0, we can determine $\langle\sigma_{g^+}\rangle$ and $\langle\sigma_{g^-}\rangle$:

$$\langle\sigma_{g^+}\rangle = (-1/\pi)\ln(1 - \langle I^+(\pi)\rangle \times \gamma_g\langle C\rangle/\langle I^0(\pi)_{\rm mes}\rangle), \tag{14}$$

$$\langle\sigma_{g^-}\rangle = (-1/\pi)\ln(1 - \langle I^-(\pi)\rangle \times \gamma_g\langle C\rangle/\langle I^0(\pi)_{\rm mes}\rangle). \tag{15}$$

If we call $\langle N^+\rangle$ the ratio $\langle I^+(\pi)\rangle/\langle I^0(\pi)_{\rm mes}\rangle$ and $\langle N^-\rangle$ the ratio $\langle I^-(\pi)\rangle/\langle I^0(\pi)_{\rm mes}\rangle$, our expressions become

$$\langle\sigma_{g^+}\rangle = (-1/\pi)\ln(1 - \gamma_g\langle C\rangle\langle N^+\rangle), \tag{16}$$

$$\langle\sigma_{g^-}\rangle = (-1/\pi)\ln(1 - \gamma_g\langle C\rangle\langle N^-\rangle). \tag{17}$$

The linearity of the measured signals with target pressure was checked for each gas studied, and the pressure of 2×10^{-4} Torr was chosen to ensure that we worked in the single-collision region and to obtain ion signals sufficiently high to be well detected by the Cary 401 electrometers. There was no background (zero pressure in target cell) signal detectable by the electrometers.

2. *Electron-loss and electron-capture cross sections for H ($2\,^2S$) atoms*

When the metastable fraction of the neutral beam is not quenched before entering the target-gas cell, Eqs. (7) and (8) become, respectively,

$$I'^+(\pi) = I^0_g(1 - e^{-\sigma_{g^+}\pi}) + I^0_m(1 - e^{-\sigma_{m^+}\pi}) = I^0[(1-F)(1 - e^{-\sigma_{g^+}\pi}) + F(1 - e^{-\sigma_{m^+}\pi})], \tag{18}$$

$$I'^-(\pi) = I^0_g(1 - e^{-\sigma_{g^-}\pi}) + I^0_m(1 - e^{-\sigma_{m^-}\pi}) = I^0[(1-F)(1 - e^{-\sigma_{g^-}\pi}) + F(1 - e^{-\sigma_{m^-}\pi})], \tag{19}$$

where F is the fraction of neutral atoms which enter the gas cell in the $2\,^2S$ state.

In the same manner as in the case of ground-state atoms, we define an average neutral correction factor when the metastable atoms are not quenched:

$$\langle C_m\rangle = \langle I'^0(\pi)\rangle/\langle I'^0(0)\rangle, \tag{20}$$

where $I'^0(\pi)$ is the neutral beam intensity with gas in the cell and $I'^0(0)$ the neutral beam intensity without gas in the cell, when atoms in the $2\,^2S$ state are not quenched. $I'^0(\pi)_{\rm mes}$, $I'^+(\pi)$, and $I'^-(\pi)$ are measured simultaneously, and alternately with $I^0(\pi)_{\rm mes}$, $I^+(\pi)$, and $I^-(\pi)$, 10 times each. As in the case of ground-state atoms, averaging the values of $I'^0(\pi)_{\rm mes}$, $I'^+(\pi)$, and $I'^-(\pi)$ over the set of data enables us to determine $\langle\sigma_{m^+}\rangle$ and $\langle\sigma_{m^-}\rangle$ from Eqs. (18) and (19):

$$\langle\sigma_{m^+}\rangle = (-1/\pi)\ln[1 - \gamma_g\langle C_m\rangle\langle N^+_m\rangle/F + (1/F - 1)\gamma_g\langle C\rangle\langle N^+\rangle], \tag{21}$$

$$\langle\sigma_{m^-}\rangle = (-1/\pi)\ln[1 - \gamma_g\langle C_m\rangle\langle N^-_m\rangle/F + (1/F - 1)\gamma_g\langle C\rangle\langle N^-\rangle], \tag{22}$$

where $\langle N^+_m\rangle$ is the ratio $\langle I'^+(\pi)\rangle/\langle I'^0(\pi)_{\rm mes}\rangle$ and $\langle N^-_m\rangle$ the ratio $\langle I'^-(\pi)\rangle/\langle I'^0(\pi)_{\rm mes}\rangle$. The values of F in Eqs. (21) and (22) obtained directly from our data,[15] vary from 0.5 at 0.5 keV to 0.25 at 3 keV. The same secondary emission coefficient γ_g is used for the ground state and the metastable parts of the neutral beam, because as in Ref. 15, we found no difference between γ_g and γ_m.

3. Deexcitation cross sections for H(2 ^2S) atoms

These cross sections cannot be measured directly in our experiment. Assuming that our data for total quenching, electron-loss and electron-capture cross sections are almost free from scattering, we can deduce the deexcitation cross sections σ_{mg} from

$$\sigma_{mg} = \sigma_T - (\sigma_{m+} + \sigma_{m-}), \tag{23}$$

where σ_T is the total quenching cross section previously measured.[18,19]

C. Errors

For the measurements of σ_{g+} and σ_{g-}, the error bars shown on our data include all sources of uncertainty such as the 20% error over γ_g. For cross sections σ_{m+} and σ_{m-} the error bars include all sources of uncertainty such as the 20% error over γ_g and the 35% error over the metastable fraction F. In order to recalibrate our values of σ_{m+} and σ_{m-} if better values of F were available, the values of F used for this work are given in Table I. The statistical error for σ_{g+}, σ_{m+}, σ_{g-}, and σ_{m-} varies typically from 5% to 10% according to the cross section measured, the gas studied, and the energy. The total error is typically 30% for σ_{g+}, 35% for σ_{g-}, 45% for σ_{m+}, and 47% for σ_{m-}. In the case of σ_{mg} the error bars have been calculated by

$$\Delta\sigma_{mg} = \Delta\sigma_{m+} + \Delta\sigma_{m-} + \Delta\sigma_T .$$

Several measurements have been made in various times and conditions, the reproducibility of which leads us to assume that a systematic error is improbable. The H^+, H^-, and H^0 intensities have been measured with Cary 401 electrometers checked against a Keithly 261 current source in order to avoid errors in the measured intensities. As the statistical error over our data is between 5% and 10%, the two important sources of uncertainty in our measurements are γ_g and F.

TABLE I. The metastable fraction F contained in the neutral beam versus the neutral beam energy.

Energy (eV)	F	Energy (eV)	F
500	0.55	1500	0.37
600	0.48	1700	0.37
700	0.42	2000	0.32
800	0.33	2200	0.30
900	0.32	2500	0.27
1000	0.30	2700	0.25
1200	0.33	3000	0.25

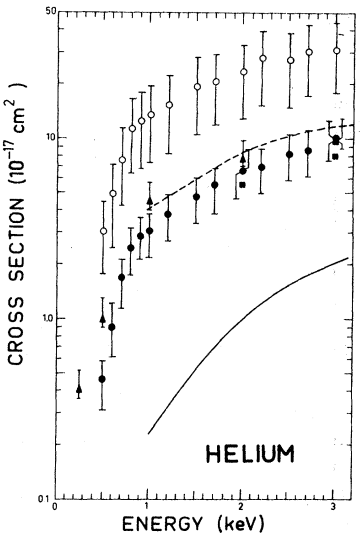

FIG. 2. Electron-loss cross sections for H(1 ^2S) and H(2 ^2S) in helium (55-mrad detector's acceptance angle). σ_{g+}: ⧳, present work; ■, Williams[5]; ▲, Smith *et al.*[9]; ——, theoretical calculation by Levy.[12] σ_{m+}: ⧲, present work; ---, theoretical calculation by Levy.[13]

III. RESULTS

A. Electron-loss cross sections

Our measurements of σ_{g+} and σ_{m+} for hydrogen in collisions with rare gases and molecular hydrogen are shown in Figs. 2–7 for a detector acceptance angle of 55 mrad. Our results for helium are consistent with those of Smith *et al.*[9] and of Williams[5] for σ_{g+}. Theoretical calculations by

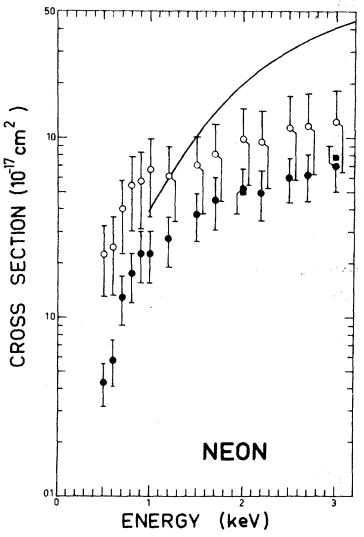

FIG. 3. Electron-loss cross sections for H(1 ^2S) and H(2 ^2S) in neon (55-mrad detector's acceptance angle). σ_{g+}: ⧳, present work; ■, Williams[5]; ——, theoretical calculation by Levy.[12] σ_{m+}: ⧲, present work.

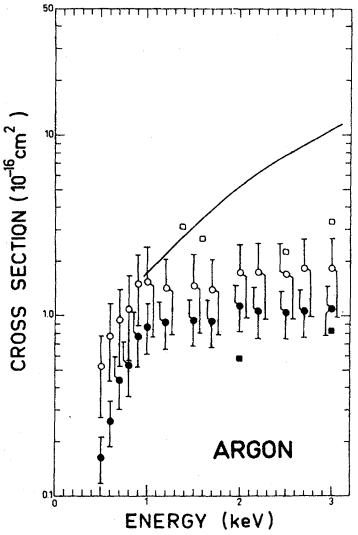

FIG. 4. Electron-loss cross sections for H(1 ^{2}S) and H(2 ^{2}S) in argon (55-mrad detector's acceptance angle). σ_{g^+}: ⧓, present work; ■, Williams[5]; ——, Levy.[12] σ_{m^+}: ⧖, present work; □, Dose and Gunz[6] recalibrated.

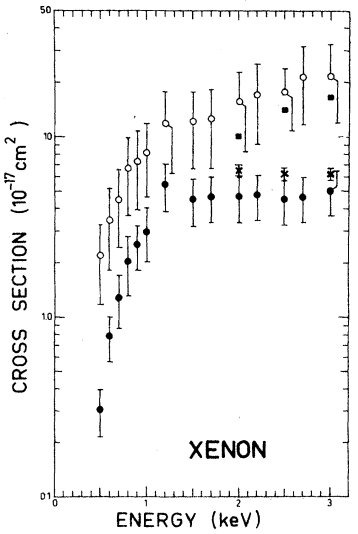

FIG. 6. Electron-loss cross sections for H(1 ^{2}S) and H(2 ^{2}S) in xenon (55-mrad detector's acceptance angle). σ_{g^+}: ⧓, present work; ■, Williams[5]; ⧗, Morgan *et al.*[11] σ_{m^+}: ⧖, present work.

Levy[12,13] are too low by factors of 5–10 for σ_{g^+} and 2.5–3.5 for σ_{m^+}. For neon our results are in good agreement with previous measurements reported by Williams[5] at 2 and 3 keV. The theoretical curve of Levy[12] for σ_{g^+} is too high by a factor of 2.2–7. Our measurements for argon differ from those of Williams by a factor of 2 at 2 keV, while at 3 keV our results are consistent with his but the slopes are different. Theoretical calculations by Levy for argon are in disagreement with our data both in values and in slope. Results of Dose and Gunz[6] for σ_{m^+} shown in Fig. 4 have been recalibrated using our values for σ_{g^+}. Figure 5 shows our data for krypton, which are in relatively good agreement with previous results of Williams. Theoretical calculations by Levy are too high by a factor of 10. Results for xenon are shown in Fig.

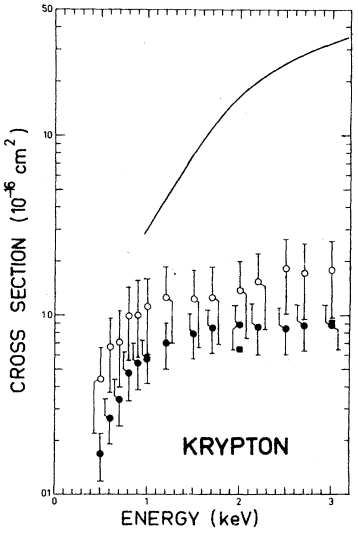

FIG. 5. Electron-loss cross sections for H(1 ^{2}S) and H(2 ^{2}S) in krypton (55-mrad detector's acceptance angle). σ_{g^+}: ⧓, present work; ■, Williams[5]; ——, Levy.[12] σ_{m^+}: ⧖, present work.

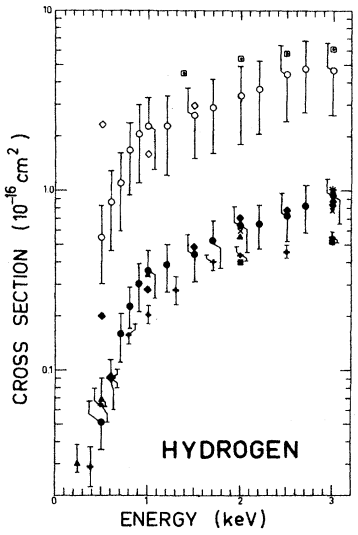

FIG. 7. Electron-loss cross sections for H(1 ^{2}S) and H(2 ^{2}S) in molecular hydrogen (55-mrad detector's acceptance angle). σ_{g^+}: ⧓, present work; ■, Williams[5]; ▲, Smith *et al.*[9]; ×, McClure[4]; ◆, Donnally and Sawyer[20]; *, Stier and Barnett[2]; ⧺, Noda.[10] σ_{m^+}: ⧖, present work; ◇, Donnally and Sawyer[20]; ⊡, Dose and Gunz.[6]

6. The data for σ_{g^+} agree quite well with those of Morgan *et al.*,[11] but the disagreement between our data and those of Williams is far outside the estimated uncertainties of the two experiments. Figure 7 shows our results for molecular hydrogen. The data for σ_{g^+} are in good agreement at 3 keV with previous measurements by Stier and Barnett,[2] and at 2 and 3 keV with data of McClure.[4] Results of Smith *et al.*[9] and of Donnally and Sawyer[20] agree well with our measurements, whereas the results of Williams[5] are within a factor of 2 below our values. Recently reported results of Noda[10] are consistent with our data at low energy but lie within a factor of 2 below our values at 3 keV. For σ_{m^+} our results are consistent with those of Donnally and Sawyer[20] except at 0.5 keV. This could be partially explained by the fact that the value of the metastable fraction of the beam was assumed by Donnally and Sawyer to be 0.25 over the whole energy range. Results of Dose and Gunz[6] are higher than our measurements, although there is no discrepancy between our values of σ_{g^+} and those of McClure against which the data of Dose and Gunz are normalized.

One can note that the ratio $\sigma_{m^+}/\sigma_{g^+}$ decreases with increasing energy for all the gases studied and that the maximum value obtained for this ratio decreases with increasing atomic number of the gas studied. An exception is xenon, where the ratio is the greatest for the rare gases. The disagreement between our results and the theoretical calculations by Levy can be explained by the fact that the Born wave calculation is not valid at low energies. It thus appears that the theoretical problem of electron loss is not solved and a theoretical model still needs to be found.

B. Electron capture cross sections

Our measurements of electron-capture cross sections for hydrogen atoms in the metastable $2\,^2S$ state and in the ground state in collisions with the rare gases and molecular hydrogen are shown in Figs. 8–13. Although the agreement between our results for σ_{g^-} and the previous measurements of Williams[5] is quite good for helium and neon, the discrepancy observed for argon, krypton, and xenon cannot be explained by experimental methods. For the case of xenon, our results which agree well with those of Morgan *et al.*,[11] show that the maximum value of σ_{g^-} is obtained for an H^+ energy of 3.5 keV. The shape of the energy dependence for hydrogen is in good agreement with previous measurements reported by McClure[4] and Williams,[5] but the values found are a factor of 1.5 above results of McClure and a factor of 2 above those of Williams. For σ_{m^-}, the results of

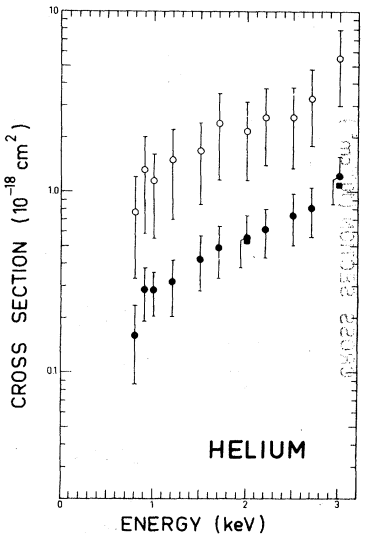

FIG. 8. Electron-capture cross sections for $H(1\,^2S)$ and $H(2\,^2S)$ in helium (55-mrad detector's acceptance angle). σ_{g^-}: ⧫, present work; ■, Williams.[5] σ_{m^-}: ⧲, present work.

Dose and Gunz[7] for argon plotted in Fig. 10 have been recalibrated against our values of σ_{g^-}. Our data are lower than theirs by a factor of 2. This discrepancy could be partially explained by the experimental procedure used by Dose and Gunz, who used calibrations against previously measured cross sections. The reproducibility of the results around 1 keV for σ_{g^-} in the case of helium, neon, krypton, and molecular hydrogen allows us to conclude that σ_{g^-} contains some structure at this en-

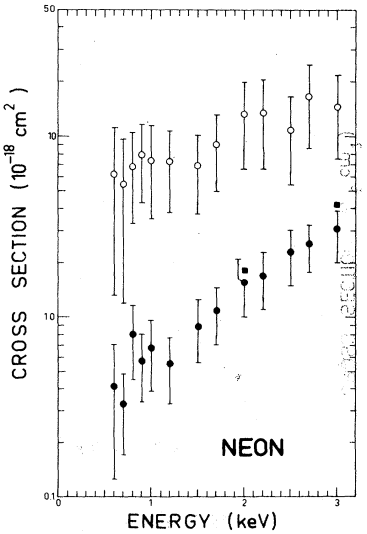

FIG. 9. Electron-capture cross sections for $H(1\,^2S)$ and $H(2\,^2S)$ in neon (55-mrad detector's acceptance angle). σ_{g^-}: ⧫, present work; ■, Williams.[5] σ_{m^-}: ⧲, present work.

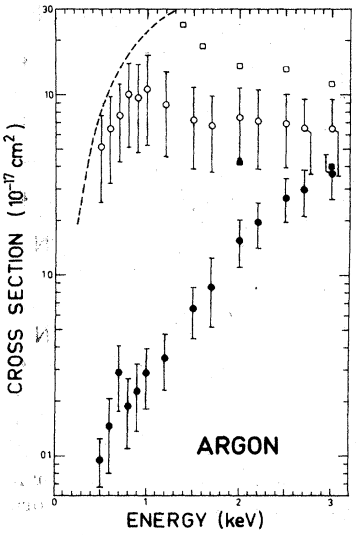

FIG. 10. Electron-capture cross sections for H(1 ^2S) and H(2 ^2S) in argon (55-mrad detector's acceptance angle). σ_g-: ⧲, present work; ■, Williams.[5] σ_m-: ⧲, present work; □, Dose and Gunz[7] recalibrated; ---, theoretical calculation by Olson.[14]

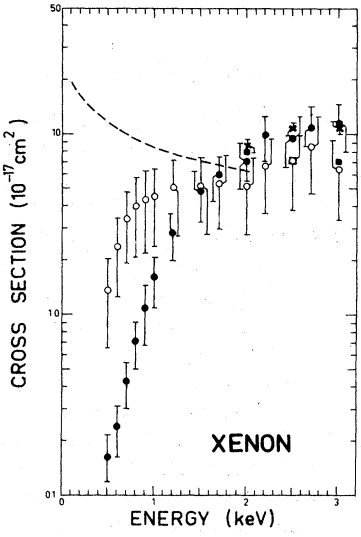

FIG. 12. Electron-capture cross sections for H(1 ^2S) and H(2 ^2S) in xenon (55-mrad detector's acceptance angle). σ_g-: ⧲, present work; ■, Williams[5]; ⧲, Morgan *et al.*[11] σ_m-: ⧲, present work; ---, Olson.[14]

ergy, even though the size of the bump is much smaller than the size of the error bars (but not if we consider only the statistical error). The structure for σ_m- is more evident. Except for helium, σ_m- presents a first bump around 1 keV and a second between 2 and 3 keV according to the gas studied.

Theoretical calculations of σ_m- by Olson[14] in the case of argon, krypton, and xenon do not describe well the energy dependence and the values of the cross section. This may be explained by the fact that the process $H(2\,^2S)+X \rightarrow H^- + X^+$ cannot be treated with a simple Landau-Zener calculation because of the presence of the $2\,^2P$ state which give rise to a second crossing point too close to the first one to be treated independently. Interferences may occur, which can decrease the value of the cross section. Furthermore, deexcitation to the ground state

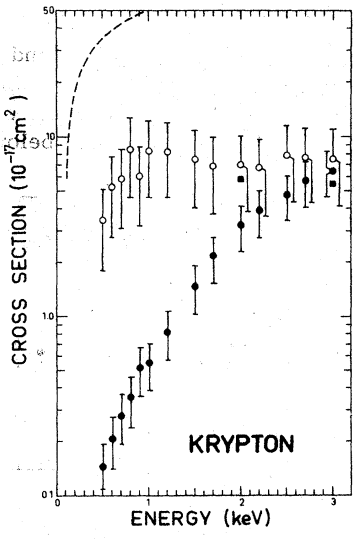

FIG. 11. Electron-capture cross sections for H(1 ^2S) and H(2 ^2S) in krypton (55-mrad detector's acceptance angle). σ_g-: ⧲, present work; ■, Williams.[5] σ_m-: ⧲, present work; ---, Olson.[14]

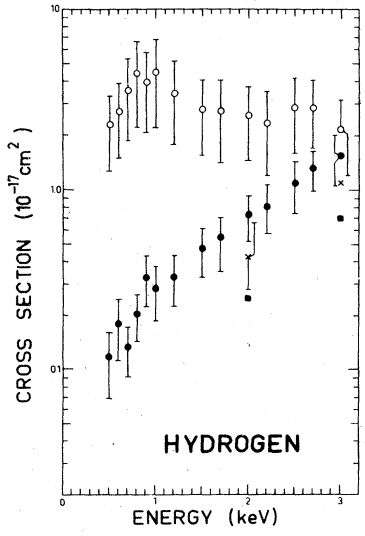

FIG. 13. Electron-capture cross sections for H(1 ^2S) and H(2 ^2S) in molecular hydrogen (55-mrad detector's acceptance angle). σ_g-: ⧲, present work; ■, Williams[5]; ×, McClure.[4] σ_m-: ⧲, present work.

is a competitive process which must be taken into account.

C. Deexcitation cross sections

Deexcitation cross sections σ_{mg} for $H(2\,^2S)$ atoms in collisions with rare gases and molecular hydrogen are shown in Figs. 14–16. These cross sections have not been measured directly as said in Sec. II B 3. Except for helium and neon, this cross section appears to be the major contribution to total quenching cross sections for $H(2\,^2S)$. The value of σ_{mg} is nearly constant over the energy range 1–3 keV for argon, krypton, and molecular hydrogen, while for helium, neon, and xenon the cross sections decreases slowly with increasing energy for $H(2\,^2S)$. In Fig. 14, theoretical calculations for the $2S$-$2P$ transition by Byron and Gersten[21] and for total deexcitation, by Levy[13] are plotted for helium. There is a factor of about 2 between our values and their predictions. Under 0.5 keV, σ_{mg} is almost equal to the total quenching cross sections previously reported,[18,19] since σ_{m^+} and σ_{m^-} are negligible for these low energies. In the case of helium, σ_{m^-} is very small and has been neglected under 0.8 keV for the calculation of σ_{mg}.

D. Scattering corrections

As the deflection system of the analyzed ions is focusing in one direction, the average acceptance angles of the products depends on the detector diameter and on the diameter of the first limiting diaphragm before the deflection area. In this experiment a reasonable choice was to take as an average acceptance angle (half angle) $\theta_1 = 57.5$ mrad; the geometric average between the acceptance of the detector (55 mrad) and the one of the next limiting diaphragm (60 mrad). Previous measurements[30] of σ_{g^+}, σ_{m^+}, σ_{g^-}, and σ_{m^-} with a smaller average acceptance angle $\theta_2 = 15$ mrad are compared with the present data in Tables II–IV. For each type of cross section the influence of scattering outside the detector can be quantitatively estimated by the corresponding collection efficiency R:

$$R = (\sigma)_0^{\theta_2}/(\sigma)_0^{\theta_1}, \tag{24}$$

where the notation $(\sigma)_0^{\theta}$ means the differential cross section is integrated over the acceptance θ:

$$(\sigma)_0^{\theta} = 2\pi \int_0^{\theta} \frac{d\sigma}{d\Omega} \sin\theta \, d\theta. \tag{25}$$

As an example, the values of $(\sigma_{g^+})_0^{\theta_1}$ and $(\sigma_{g^+})_0^{\theta_2}$ for He are compared in Fig. 17. From Tables II–IV it is seen that the collection efficiencies remain fairly close to 1 except at energies below 1 keV

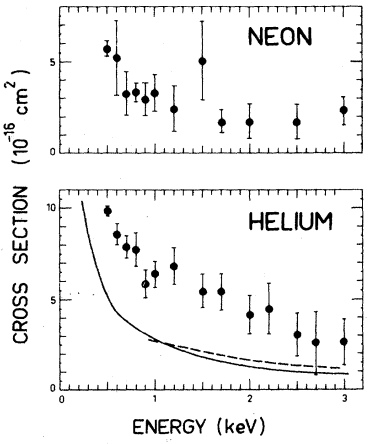

FIG. 14. Deexcitation cross section for $H(2\,^2S)$ in helium and neon: ⧓, present work; ——, theoretical calculation by Byron and Gersten[21]; ---, theoretical calculation by Levy.[13]

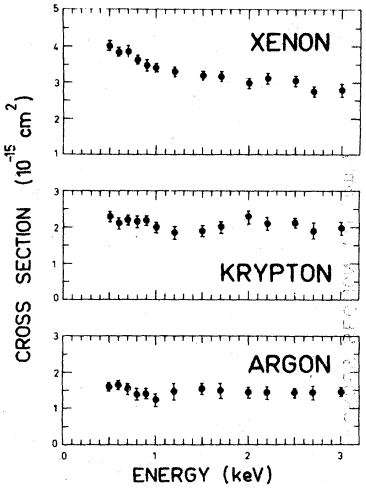

FIG. 15. Deexcitation cross sections for $H(2\,^2S)$ in argon, krypton, and xenon: ⧓, present work.

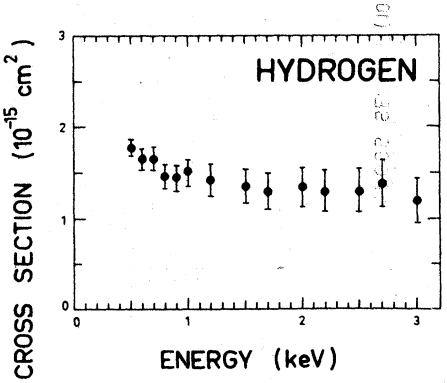

FIG. 16. Deexcitation cross section for $H(2\,^2S)$ in molecular hydrogen: ⧓, present work.

TABLE II. Comparison of cross sections measured with a 15-mrad acceptance detector and a 57.5-mrad acceptance detector—helium.

Energy (keV)	$H(1^2S) \rightarrow H^+$ $\sigma_{g^+}(10^{-17}\ cm^2)$ $\theta_1 = 57.5$ mrad	$\theta_2 = 15$ mrad	R	R'	σ_{g^+} corrected for scattering (see Ref. 22)	$H(2^2S) \rightarrow H^+$ $\sigma_{m^+}(10^{-16}\ cm^2)$ $\theta_1 = 57.5$ mrad	$\theta_2 = 15$ mrad	R
0.5	0.46	0.05	0.11			0.31	0.08	0.25
1.0	3.06	2.58	0.84	0.91	3.36	1.36	1.61	1.18
1.5	4.74	4.58	0.97			1.93	1.82	0.94
2.0	6.76	6.07	0.90	0.94	7.17	2.35	2.23	0.95
2.5	8.34	8.97	1.08			2.73	2.84	1.04
3.0	10.1	9.98	0.99			3.10	3.44	1.11

where the influence of scattering becomes considerable and cannot be neglected, especially for the cross sections σ_{g^+}. Before calculating a correction some remarks should be made concerning the order of magnitude of the scattering in the present measurements by a comparison between the different collection efficiencies:

(a) For given energy, projectile and target gas, the scattering of H^- is not so pronounced as the one of H^+, showing that the effects on σ_{g^-} and σ_{m^-} are lower than those on σ_{g^+} and σ_{m^+}, respectively.

(b) For a given energy, target gas, and process, the scattering of the ions is more pronounced when they are formed from $H(1^2S)$ rather than from $H(2^2S)$. This point is easy to understand since the outgoing ions spend less time in the interaction potential when they are formed from $H(2^2S)$.

(c) The effect of scattering increases with the mass of the target gas.

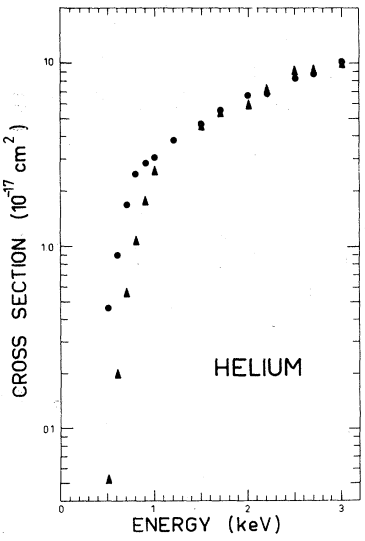

FIG. 17. Scattering effects over σ_{g^+} in helium: ●, present work, 57.5 mrad acceptance angle; ▲, data of Ref. 30, 15-mrad acceptance angle.

(d) At first sight it seems that the measurements of σ_{m^+} and σ_{m^-} could be affected by the collection efficiencies corresponding to σ_{g^+} and σ_{g^-}. In fact it is easy to show from Eqs. (7), (8), (18), and (19) that the scattering error over σ_{g^+} and σ_{g^-} are eventually eliminated in the determination of σ_{m^+} and σ_{m^-}. In other words, there is no interference between the scattering corrections, and the collection efficiencies are independent.

Fleischmann *et al.*[22] have measured the scattering up to 7° in stripping collisions of $H(1^2S)$ in He, Ar, Kr, and H_2 at energies as low as 1 keV. They have estimated the collection efficiencies at 7° and their results are normalized to total stripping cross sections obtained by Stier and Barnett,[2] Williams,[5] and Solov'ev *et al.*[23] The collection efficiencies in Tables II–IV are consistent with scattering data of Fleischmann *et al.* This agreement is independent of any normalization since only ratios of cross sections are needed to calculate the collection efficiencies. Having fulfilled this condition, the data of Fleischmann *et al.* have been used to calculate new collection efficiencies:

$$R' = \frac{(\sigma)_0^{\theta_1}}{(\sigma)_0^{\theta_3}} \frac{(\sigma)_0^{\theta_3}}{(\sigma)_0^{\theta_4}} = \frac{(\sigma)_0^{\theta_1}}{(\sigma)_0^{\theta_4}} \tag{26}$$

with $\theta_1 = 57.5$ mrad (present acceptance angle), $\theta_3 = 7°$ (acceptance angle of Ref. 22), and $\theta_4 \sim \pi$. When the scattering outside 7° is small (e.g., He) the second term in R' is very close to 1. For Kr at 1 keV, the second term is 0.75, indicating that even with an acceptance angle of 7°, 25% of the H^+ ions are scattered outside the detector at 1 keV. The calculated values of R' at 1 and 2 keV are given in Tables II–IV for He, Ar, and H_2. In the case of krypton, the values of R' are 0.60 at 1 keV and 0.64 at 2 keV. The corresponding corrected values for σ_{g^+} are 9.44×10^{-17} at 1 keV and 1.47×10^{-16} at 2 keV.

In conclusion, according to the data of Fleischmann *et al.*,[22] it appears that the present measured values of σ_{g^+} at 1 keV is too low by 9% in He, by

TABLE III. Comparison of cross sections measured with a 15-mrad acceptance detector and a 57.5-mrad acceptance detector—argon.

Energy (keV)	$H(1^2S) \rightarrow H^+$ $\sigma_{g^+}(10^{-17}\ cm^2)$ $\theta_1 = 57.5$ mrad	$\theta_2 = 15$ mrad	R	R'	σ_{g^+} corrected for scattering (see Ref. 22)	$H(2^2S) \rightarrow H^+$ $\sigma_{m^+}(10^{-16}\ cm^2)$ θ_1	θ_2	R	$H(1^2S) \rightarrow H^-$ $\sigma_{g^-}(10^{-18}\ cm^2)$ θ_1	θ_2	R	$H(2^2S) \rightarrow H^-$ $\sigma_{m^-}(10^{-17}\ cm^2)$ θ_1	θ_2	R
0.5	1.63	0.33	0.20			0.52	0.20	0.39	0.95	0.25	0.26	5.06	1.58	0.31
1.0	8.65	4.99	0.58	0.77	11.2	1.54	1.43	0.93	2.83	3.11	1.10	10.7	10.7	1.00
1.5	9.53	8.38	0.88			1.47	1.51	1.03	6.47	6.20	0.96	7.36	7.87	1.07
2.0	11.4	9.47	0.83	0.84	13.5	1.73	1.58	0.91	15.5	15.3	0.99	7.56	6.90	0.91
2.5	10.5	11.1	1.06			1.70	1.69	0.99	26.8	26.6	0.99	6.90	6.70	0.97
3.0	11.0	11.0	1.00			1.84	2.02	1.10	36.4	35.8	0.99	6.49	6.30	0.97

TABLE IV. Comparison of cross sections measured with a 15-mrad acceptance detector and a 57.5-mrad acceptance detector—molecular hydrogen.

Energy (keV)	$H(1^2S) \rightarrow H^+$ $\sigma_{g^+}(10^{-17}\ cm^2)$ $\theta_1 = 57.5$ mrad	$\theta_2 = 15$ mrad	R	R'	σ_{g^+} corrected for scattering (see Ref. 22)	$H(2^2S) \rightarrow H^+$ $\sigma_{m^+}(10^{-16}\ cm^2)$ θ_1	θ_2	R	$H(1^2S) \rightarrow H^-$ $\sigma_{g^-}(10^{-18} cm^2)$ θ_1	θ_2	R	$H(2^2S) \rightarrow H^-$ $\sigma_{m^-}(10^{-17}\ cm^2)$ θ_1	θ_2	R
0.5	0.52	0.087	0.17			0.56	0.32	0.57	1.15	0.50	0.43	2.28	1.85	0.81
1.0	3.54	2.55	0.72	0.94	3.78	2.27	2.24	0.99	2.82	2.87	1.02	4.42	5.12	1.16
1.5	4.39	4.53	1.03			2.61	2.87	1.10	4.68	4.82	1.03	2.78	3.24	1.17
2.0	6.32	6.23	0.99	0.96	6.61	3.38	3.34	0.99	7.25	7.31	1.01	2.56	2.46	0.96
2.5	7.37	7.55	1.02			4.41	4.16	0.94	10.8	10.5	0.97	2.84	2.30	0.81
3.0	9.04	8.72	0.96			4.62	4.36	0.94	15.3	14.0	0.92	2.14	2.21	1.03

23% in Ar, by 39% in Kr, and by 6% in H_2. Although a reliable correction has been calculated in 1 keV, it is not possible to deduce from it a correction at lower energy. No scattering data have been found to adjust the cross sections σ_{m^+}, σ_{g^-}, and σ_{m^-}. Although the corrections are certainly less considerable for these cross sections, it must be kept in mind, for an eventual comparison with theoretical prediction, that the present measured quantities are $(\sigma)_0^{57.5\ \mathrm{mrad}}$, and not the total cross sections. A precise measurement of these total cross sections would need additional experimental information about the scattering of the ions formed by electron loss or by electron capture of $H(2\,^2S)$ and $H(1\,^2S)$ in collisions with noble gases.

E. Highly excited states

The presence in the neutral beam of hydrogen atoms in highly excited states with $n \geq 3$ can contribute to the positive ion signal during the measurements of σ_{g^+}. Although the distribution among these states decreases rapidly when n increases, the corresponding ionization cross sections, in collisions with the target gas, can be very large. The hydrogen excited states formed in the cesium cell are separated into three groups according to the principal quantum number n:

a. $3 \leq n \leq 6$. As discussed in Sec. II A, the distance between the cesium target and the gas target cell is long enough to ensure that, even at 3 keV, essentially all the excited atoms decay to the ground state or to the metastable state $H(2\,^2S)$. No contribution is expected from these states.

b. $n \geq 15$. In order to eliminate the contribution of the higher excited states, a 15-kV/cm electric field was applied between two grids 1 mm apart and located at the exit of the cesium cell (Fig. 1). The field ionization probabilities of hydrogen excited states are well known from the work of Bailey *et al.*[24] The electric field required to ionize an excited state varies as n^{-4} and all the states with $n \geq 15$ are field ionized by the grids. The created protons are then eliminated by the sweeping plates. When the ionizing electric field was turned on, with Ar as target gas, the variation of the positive ion signal was not detectable for all energies between 0.5 and 3 keV. As it is possible to detect a 1% variation of the signal, we conclude that the contribution of the higher excited states ($n \geq 15$) is negligible. At 0.5 keV the electron-loss cross section for $H(1\,^2S)$ colliding with Ar is 1.6×10^{-17} cm^2. Thus the product of the fraction of higher excited states with $n \geq 15$ in the neutral beam and the averaged ionization cross section of these states in Ar is smaller than 1.6×10^{-19} cm^2. Dixon *et al.*[25] have observed a background positive ion signal while measuring the electron impact ionization cross sections for $H(2\,^2S)$ atoms formed in a Cs target at 2 keV. The signal was attributed to Lorentz ionization of highly excited states ($n > 37$) in the magnetic field of the analyzer magnet. This result is not in contradiction with our conclusion, because the thickness of our gas target, which is of the order of 5×10^{13} atoms/cm^2, is about 10^4 times larger than the equivalent thickness of the electron beam target used in the experiment of Dixon *et al.* Our positive ion signal, due to the electron loss of $H(1\,^2S)$, would then be expected to be much larger than the background signal observed by Dixon *et al.* in a counting mode.

c. $7 \leq n \leq 14$. The neutral beam still contains some excited states which are not destroyed by the ionizing electric field and can contribute to the positive ion signal. Il'in *et al.*[26] have measured the cross sections for the formation of excited states with $9 \leq n \leq 16$ in collisions between protons and cesium at energies down to 10 keV and have verified the n^{-3} dependence, as theoretically predicted by Hiskes.[27] Although it is possible to extrapolate these data down to a few keV, the lack of ionizing cross section data for these states prevents any attempt to calculate a correction. However, the method of formation of the primary $H(1\,^2S)$ atoms varies greatly among the experiments where the electron-loss cross section σ_{g^+} was measured. It is unlikely that these methods would give the same population distribution over the excited states with $7 \leq n \leq 14$ because the energy defects are not the same. Despite the different methods of formation of $H(1\,^2S)$, however, a comparison of the results for the same target gas at 3 keV, where the scattering effects are reduced, does not show any significant deviation. For all the target gases, except Xe, the standard deviation, resulting from the dispersion of the different measurements, is lower or equal to our experimental uncertainty. Thus we can conclude that the effect of the high excited states is negligible in our measurements of σ_{g^+}.

IV. DISCUSSION OF THE ELECTRON-CAPTURE CROSS SECTIONS

Although the interpretation of the electron-capture cross sections depends on the details of the potential curves for each system, it is interesting to make some general comments concerning the ratio of the two electron-capture cross sections $\rho = \sigma_{m^-}/\sigma_{g^-}$. This ratio is of practical importance in the efficiency of the H^- polarized ion sources where the H^- ions created from the ground-state atoms of the neutral beam are not polarized. For a target gas X, the electron capture from $H(2\,^2S)$

TABLE V. Ionization potential (I_x) energy defect (Δ_m) and Landau-Zener parameter (W_m) for the process $H(2\,^2S)+X \rightarrow H^-+X^+$.

Gas	I_x (eV)	Δ_m (eV)	W_m 0.5 keV	1 keV	2 keV	3 keV
He	24.46	13.57	6.84	4.84	3.42	2.79
Ne	21.47	10.58	6.10	4.32	3.05	2.49
Ar	15.68	4.79	0.69	0.49	0.34	0.28
Kr	13.93	3.04	0.022	0.016	0.012	0.009
Xe	12.08	1.19	$<10^{-3}$	$<10^{-3}$	$<10^{-3}$	$<10^{-3}$

occurs at the diabatic intersection of the ionic potential curve H^-+X^+ with the covalent potential curve $H(2\,^2S)+X$. The crossing radius R_{xm} may be approximated by $1/\Delta_m$ where Δ_m is the difference between the ionization potential I_X of X and the electron affinity of $H(2\,^2S)$(10.9 eV). The electron capture from $H(1\,^2S)$ occurs at a crossing radius $R_{Xg}<R_{Xm}$ since the entrance channel $H(1\,^2S)+X$ is 10.2 eV lower than the channel $H(2\,^2S)+X$. The exit channel H^-+X^+ crosses the infinite series of excited states $H+X^*$ and $H(n>2)+X^*$.[14] A straightforward analysis within the framework of a Landau-Zerner formalism shows that in first approximation ρ is independent of the crossings with the excited states and can be expressed as

$$\rho=(1-e^{-W_m})\left[\left(\frac{R_{Xm}}{R_{Xg}}\right)^2\frac{1}{e^{-W_g}(1-e^{-W_g})}-1\right], \qquad (27)$$

where W_m and W_g are the well-known Landau-Zener parameters at the two crossing points R_{Xm} and R_{Xg}. This relation shows that ρ can become less than unity only when the Landau-Zener parameter W_m is much smaller than unity, the target gas X being in that case a very poor candidate for polarized ion sources. Xenon is the only target gas which exhibits experimentally an energy range ($E>1.5$ keV) where $\rho<1$. At 3 keV for krypton the ratio is found very close to 1 and for all the gases ρ decreases with increasing energy above 1 keV. By using empirical coupling matrix elements obtained by Olson *et al.*[28] and Grice and Merschbach[29] we have calculated the Landau-Zener parameter W_m for all the studied target gases and for the following energies: 0.5, 1, 2, and 3 keV. The calculated values are given in Table V. It was verified that Xe and Kr have small values of W_m in our energy range and that W_m decreases with increasing energy. From this analysis it is expected that Ar will exhibit the same behavior $\rho<1$ for energies greater than 4 keV.

Olson[14] performed rough calculations of ρ at 0.5 keV for Ar, Kr, and Xe. His results are in agreement with our data for the inequality $\rho(\mathrm{Ar})>\rho(\mathrm{Kr})>\rho(\mathrm{Xe})$, but the experimental values are larger than the calculated ones by a factor of 3 for Ar, 1.4 for Kr, and 4.7 for Xe.

ACKNOWLEDGMENTS

The authors would like to thank Dr. C. Manus and Dr. G. Watel for their kind assistance, and Dr. K. A. Smith for communicating his results prior to publication.

[1]B. Donnally and W. Sawyer, Phys. Rev. Lett. 15, 439 (1965).
[2]P. M. Stier and C. F. Barnett, Phys. Rev. 103, 896 (1956).
[3]R. Curran and T. M. Donahue, Phys. Rev. 118, 1233 (1960).
[4]G. W. McClure, Phys. Rev. 134, A1226 (1964).
[5]J. F. Williams, Phys. Rev. 153, 116 (1967).
[6]V. Dose and R. Gunz, J. Phys. B 5, 636 (1972).
[7]V. Dose and R. Gunz, J. Phys. B 5, 1412 (1972).
[8]G. Spiess, A. Valance, and P. Pradel, Phys. Rev. A 6, 746 (1972).
[9]K. A. Smith, M. D. Duncan, M. W. Geis, and R. D. Rundel, J. Geophys. Res. 81, 2231 (1976).
[10]N. Noda, J. Phys. Soc. Jpn. 41, 625 (1976).
[11]T. J. Morgan, K. H. Berkner, W. G. Graham, R. V. Pyle, and J. W. Stearns, Phys. Rev. A 14, 664 (1976).
[12]H. Levy II, Phys. Rev. 185, 7 (1969).
[13]H. Levy II, Phys. Rev. A 3, 1987 (1971).
[14]R. E. Olson, Nucl. Instrum. Methods 126, 467 (1975).
[15]P. Pradel, F. Roussel, A. S. Schlachter, G. Spiess, and A. Valance, Phys. Rev. A 10, 797 (1974).
[16]P. Pradel and F. Roussel, Nucl. Instrum. Methods 121, 111 (1974).
[17]Vu Ngoc Tuan, G. Gautherin, and A. S. Schlachter, Phys. Rev. A 9, 1242 (1974).
[18]V. Dose, W. Hett, R. E. Olson, P. Pradel, F. Roussel, A. S. Schlachter, and G. Spiess, Phys. Rev. A 12, 1261 (1975).
[19]F. Roussel, P. Pradel, and G. Spiess, Phys. Rev. A 15, 451 (1977).
[20]B. Donnally and W. Sayer, in *Proceedings of the Sixth International Conference on the Physics of Electronic and Atomic Collisions, Cambridge, Mass., 1969*, edited by I. Amder (MIT Press, Cambridge, Mass., 1969).
[21]F. W. Byron, Jr. and J. I. Gersten, Phys. Rev. A 3, 620 (1971).
[22]H. H. Fleischmann, C. F. Barnett, and J. A. Ray, Phys. Rev. A 10, 569 (1974).
[23]E. S. Solov'ev, R. N. Il'in, V. A. Oparin, and N. V. Fedorenko, Zh. Eksp. Teor. Fiz. 42, 659 (1962) [Sov. Phys.-JETP 15, 459 (1962)].
[24]D. S. Bailey, J. R. Hiskes, and A. C. Riviere, Nucl. Fusion 5, 41 (1965).
[25]A. J. Dixon, A. Von Engel, and M. F. A. Harrison,

Proc. R. Soc. Lond. A 343, 333 (1975).
[26]R. N. Il'in, V. A. Oparin, E. S. Solov'ev, and N. V. Fedorenko, Zh. Tekh. Fiz. 36, 1241 (1966) [Sov. Phys. Tech. Phys. 11, 921 (1967)].
[27]J. R. Hiskes, Phys. Rev. 180, 146 (1969).
[28]R. E. Olson, F. T. Smith, and E. Bauer, Appl. Opt. 10, 1848 (1971).
[29]R. Grice and D. R. Merschbach, Mol. Phys. 27, 159 (1974).
[30]F. Roussel, P. Pradel, A. S. Schlachter, and G. Spiess, IX ICPEAC, Seattle (1975), p. 27.